RSC Advances

The influence of lateral fluorination and cyanation on the mesomorphism of polycatenar mesogens and the nature of the SmC phase therein

Journal:	*RSC Advances*
Manuscript ID:	RA-ART-08-2015-017100
Article Type:	Paper
Date Submitted by the Author:	24-Aug-2015
Complete List of Authors:	Smirnova, Antonina; Ivanovo State University, Nanomaterials Research Institute HEINRICH, Benoît; Institut de Physique et Chimie des Matériaux de Strasbourg -IPCMS, CNRS-Université de Strasbourg (UMR 7504) Donnio, Bertrand; Institut de Physique et Chimie des Matériaux de Strasbourg -IPCMS, CNRS-Université de Strasbourg (UMR 7504) Bruce, Duncan; University of York, Department of Chemistry

The influence of lateral fluorination and cyanation on the mesomorphism of polycatenar mesogens and the nature of the SmC phase therein

Antonina I. Smirnova*[a,b], Benoît Heinrich*[c], Bertrand Donnio*[c,d] and Duncan W. Bruce*[a]

[a] Department of Chemistry, University of York, Heslington, YORK, YO10 5DD, UK

E-mail: duncan.bruce@york.ac.uk

[b] Nanomaterials Research Institute, Ivanovo State University, Ermak str., 37/7, 153025 IVANOVO, RUSSIA

E-mail: antonia_smirnova@mail.ru

[c] Institut de Physique et Chimie des Matériaux de Strasbourg (IPCMS), CNRS-Université de Strasbourg (UMR 7504), 23 rue du Loess BP 43, 67034 STRASBOURG Cedex 2, FRANCE

E-mail: heinrich@ipcms.unistra.fr, E-mail: bertrand.donnio@ipcms.unistra.fr

[d] Complex Assemblies of Soft Matter Laboratory (COMPASS), CNRS-Solvay-University of Pennsylvania (UMI 3254) CRTB, 350 George Patterson Boulevard, BRISTOL, PA 19007, USA

Abstract

Several series of tetracatenar mesogens having different lateral substituents (–F, –CN, –CF_3) on the central benzene ring of the molecule have been synthesised and their mesomorphic behaviour investigated by polarising microscopy, differential scanning calorimetry and small-angle X-ray scattering methods.

The study offers an insight into the effect of different lateral polar functions on the mesomorphism of tetracatenar mesogens and starts to try to delineate polar and steric contributions. Thus –CF_3 exerts a strong steric effect that destabilises more organised mesophases (SmC, ribbon) and reduces transition temperatures. Use of a central tetrafluorophenyl unit also destabilises organised phases in common with observations made in calamitic materials, but the use of only one or two lateral fluorines has relatively little effect on transition temperatures and mesomorphism. The more polar cyano function is different in that addition of one such group reduced transition temperatures and destabilises the nematic and crystal phase, whereas the more symmetric derivative with two cyano functions shows more stable crystal and mesophases. A detailed geometrical analysis supported by X-ray diffraction data (and a dilatometry data base) leads to the proposal of a model for the SmC-to-Col_r phase transformation triggered by chain-induced layer undulations in the smectic phase.

Graphic Abstract

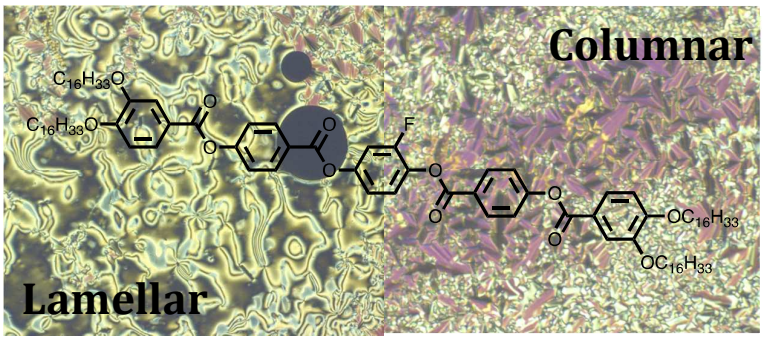

Introduction

Polycatenar liquid crystals [1,2] have been of interest for some time owing to the fact that 3,3',4,4'-terminally substituted tetracatenar mesogens tend to show nematic and SmC phases at shorter chain lengths and columnar phases at longer chain lengths. In addition, that part of the phase diagram where the change from lamellar to columnar mesomorphism occurs has attracted particular attention in order to understand what drives the change in organisation. As part of our on-going work in this area, we reported previously on the synthesis of some five-ring, tetracatenar mesogens (Figure 1) in which the central phenyl ring was partially or fully substituted by methyl groups (compounds **2-4**), and determined how their mesomorphism was affected by those substituents.[3] It was found that substitution by only one methyl group was sufficient to lead to the complete suppression of columnar order found for longer-chain (*n* = 14, 16) non-substituted homologues of the 'parent' compound **1**. The suppression of the columnar phase was explained by steric hindrance in which the lateral methyl group(s) prevented the self-organisation necessary for the phase to form. Thus, only nematic and/or smectic C phases were detected for compounds **2-4** even for long-chain homologues.

It is known that for calamitic mesogens, the use of polar lateral substituents can have a profound influence on both the nature of the mesophases seen and their transition temperatures. The most common substituent used is fluorine and while it is found occasionally that lateral fluorination can stabilise lamellar phases when used in conjunction with so-called 'outboard dipoles', for the most part they act to destabilise lamellar phases in favour of nematic phases.[4,5] Such behaviour is understood readily as a steric perturbation of the side-to-side self-organisation required in smectic phases given that the atomic radius of fluorine is some 16% greater than that of hydrogen. In addition and significantly, fluorine also introduces a significant dipole to the molecule, which has been used as a terminal dipole in newer families of display materials [6] and to realise materials with negative dielectric anisotropy in other families of display mixtures, most notably the fluoroterphenyls.[7] As exemplified by compounds **2** and **3**, larger lateral substituents can exert a significant steric effect. Cyano groups fall into this category, although there are examples of

calamitic mesogens with lateral cyano groups that exhibit negative anisotropy of their dielectric properties.[8,9,10]

Having seen that lateral methyl substituents had such a significant effect on the mesomorphism of polycatenar mesogens, it was then of interest to determine if sterically less demanding fluorine substituents, with their attendant electronic effects, would be similarly effective in suppressing columnar organisation. In addition, the larger trifluoromethyl and cyano functions were also targets of interest.

In this article we present synthesis and mesomorphic properties of five new series of tetracatenar mesogens having one (**5**-*n*), two (**6**-*n*) or four (**7**-*n*) fluorine atoms in lateral positions of the central phenyl ring as wells as examples with a CF_3-group (**8**-*n*) and one (**9**-*n*) or two (**10**-*n*) cyano groups (Figure 1).

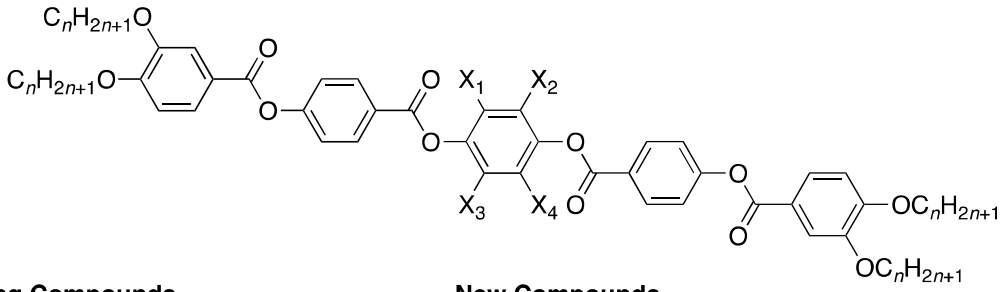

Existing Compounds
1-*n*: $X_1 - X_4 = H$
2-*n*: $X_1 = X_3 = X_4 = H$; $X_2 = Me$
3-*n*: $X_1 = X_2 = Me$; $X_3 = X_4 = H$
4-*n*: $X_1 = X_2 = X_3 = X_4 = Me$

New Compounds
5-*n*: $X_1 = X_3 = X_4 = H$, $X_2 = F$
6-*n*: $X_1 = X_2 = F$, $X_3 = X_4 = H$
7-*n*: $X_1 = X_2 = X_3 = X_4 = F$
8-*n*: $X_1 = X_3 = X_4 = H$, $X_2 = CF_3$
9-*n*: $X_1 = X_3 = X_4 = H$, $X_2 = CN$
10-*n*: $X_1 = X_2 = CN$, $X_3 = X_4 = H$

Figure 1 Molecular structures of the tetracatenar mesogens discussed previously (**1-4**)[3] or prepared (**5-10**) as part of this study.

Synthesis

The compounds investigated in this work were synthesised according to Scheme 1. Thus, 3,4-dialkoxybenzoyloxybenzoic acids [11] were esterified with the appropriate 1,4-hydroquinone using

DCC/DMAP in dichloromethane at room temperature.[3] 1,2,3,4-Tetrafluorohydroquinone and 2,3-dicyanohydroquinone were available commercially, but the hydroquinones required for **5**, **6**, **8** and **9** were prepared by literature methods (see experimental). The ^{1}H NMR spectra of the products showed the typical AMX spin system for the ring bearing the dialkoxy fragments and an AA'XX' system for the next ring towards the centre. The splitting pattern for the central ring depended on the hydroquinone used in the reaction. Yields, NMR and analytical data are collected in the Experimental section below.

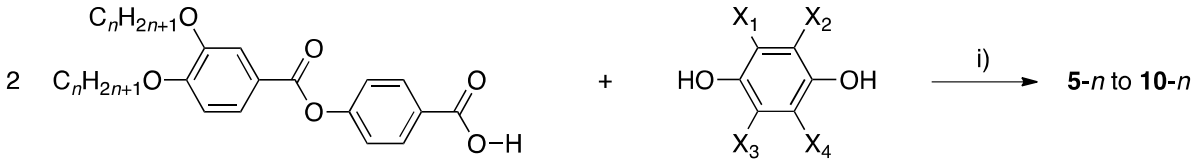

Scheme 1 Synthetic pathway for preparation of tetracatenar compounds **5**-*n* to **10**-*n*.
Conditions: i) DCC/DMAP/CH_2Cl_2/rt

Mesomorphism

The new, laterally substituted, tetracatenar mesogens were studied by polarising optical microscopy and DSC to determine their mesomorphism and transition temperatures, and then the mesophases were characterised further using small-angle X-ray scattering (SAXS). The thermal behaviour is collected in Table 1 (and in the phase diagrams in figure S1 in the SI) .

Table 1. Thermal data for the new compounds

Compound	Transition	*T*/°C	Δ*H*/kJ mol^{-1}	Δ*S*/R
5-10	Cr – SmC	148.1	68.0	161
	SmC – N	161.8	9.0	21
	N – Iso	176.4	1.1	3
5-12	Cr – Cr'	127.4	21.6	54
	Cr' – SmC	148.7	75.8	180
	SmC – N	159.1	8.0	19
	N – Iso	165.8	1.1	3
5-14	Cr – SmC	139.9	72.4	175
	SmC – N	155.1	4.6	11
	N – Iso	156.9	0.3	1
5-16†	Cr – Cr'	130.1	35.7	89
	Cr' – Col_r	133.9	50.3	124
	Col_r – Iso	152.0	9.1	22
	(SmC – Iso)	(151.0)	(6.6)	(16)
	(Col_r – SmC)	(147.3)	(0.6)	(1)

6-10	Cr – SmC	150.5	43.1	102
	SmC – N	153.9	2.7	6
	N – Iso	174.5	1.1	3
6-12	Cr – Cr'	112.1	19.6	51
	Cr' – SmC	136.7	69.1	169
	SmC – N	152.3	6.9	16
	N – Iso	164.3	1.2	3
6-14	Cr – Cr'	123.9	9.4	24
	Cr' – SmC	132.9	75.4	186
	SmC – N	149.0	5.9	10
	N – Iso	155.6	1.0	2
6-16	Cr – Cr'	122.8	36.6	92
	Cr' – SmC	129.7	82.2	204
	SmC – N	144.8	4.8	12
	N – Iso	147.7	0.6	1
7-10	Cr – Cr'	128.1	11.8	29
	Cr' – N	142.5	69.1	166
	N – Iso	153.3	1.3	3
7-12	Cr – N	134.8	64.1	157
	N – Iso	142.6	1.0	2
7-14	Cr – N	129.8	21.2	53
	N – Iso	135.9	0.8	2
	(SmC – N)	(136.3)	(1.8)	(4)
8-10	Cr – N	130.7	103.9	257
	N – Iso	144.9	1.1	3
8-12	Cr – N	129.8	111.4	277
	N – Iso	136.4	0.3	1
8-14	Cr – Iso	128.6	132.1	329
	(N – Iso)	(127.9)	(1.0)	(3)
9-10	Cr – SmC	125.2	81.9	206
	SmC – N	158.1	5.7	13
	N – I	164.1	0.9	2
9-12	Cr – SmC	128.2	104.5	260
	SmC – I	156.1	6.6	15
9-14	Cr – Col_r	128.5	123.7	308
	Col_r – SmC	146.6	0.5	1
	SmC – I	150.6	6.2	15
9-16	Cr – Cr'	106.1	2.0	5
	Cr' – Col_r	126.3	156.5	392
	Col_r – I	144.2	7.6	18
10-10	Cr – SmC	156.0	66.0	154
	SmC – N	172.3	3.8	9
	N – I	175.9	1.0	2
10-12	Cr – SmC	148.8	63.0	149
	SmC – I	164.0	4.9	11
10-14	Cr – Cr'	121.9	1.2	3
	Cr' – Col_h	130.5	50.0	124
	Col_h – I	145.9	5.0	12

† See text for discussion of the phase behaviour of this compound.

Mesomorphism of series 5

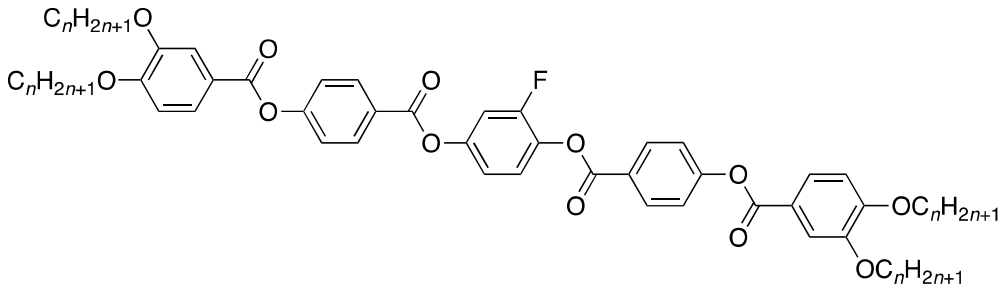

5-*n*

The first three synthesised homologues of the series **5**, namely **5**-10, **5**-12 and **5**-14, show smectic C (SmC) and nematic (N) phases. The phases were assigned by characteristic optical textures of the schlieren type (Figure 2a, c). Although both phases display very similar textures they can be easily identified due to distinct fluctuations at the phase transition (see Figure 2b). Small-angle X-ray analysis of **5**-14 between 140 and 150 °C also supported the existence of SmC phase (Table 2) and, with an estimated molecular length for **5**-14 of 70 Å, then the tilt angle is calculated to be in the range of 55-60° (see below).

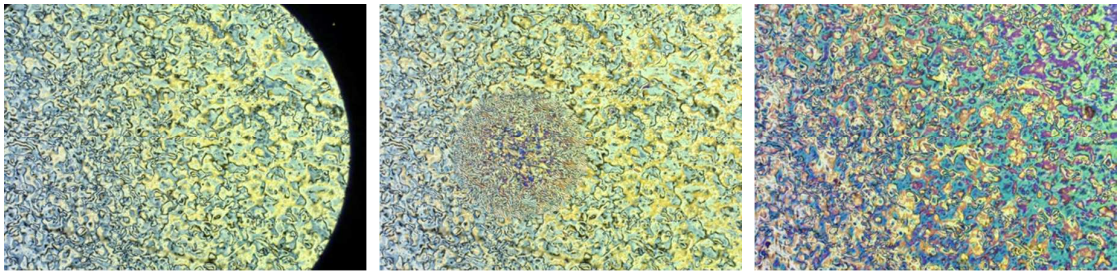

a ***b*** ***c***

Figure 2. Typical schlieren textures taken on cooling from the isotropic liquid of compound **5**-14: *a*) in the nematic phase at 157 °C; *b*) at the transition from nematic phase to SmC phase at 155 °C (the SmC grows from the centre); *c*) in the SmC phase at 140 °C.

The longest-chain term of the series, **5**-16, exhibited a completely different mesomorphism so that on heating, the compound melted to give a mesophase with small, fine fan-like texture, which appeared to extend all the way up to the clearing point. However, on cooling from the isotropic phase the schlieren texture of a SmC phase was clearly visible and this gave way to a fan texture

on slow cooling (Figure 3). Careful re-examination of the sample on heating then showed that if the compound was held isothermally just below the clearing point, then the fan texture slowly gave way to a schlieren texture. This is not observed even on heating at 1 K min^{-1} and shows a very strong paramorphosis – indeed it is not possible to see a defined transition on heating (neither by microscopy nor DSC) and for that reason no formal Col_r–SmC transition temperature is recorded in Table 1. Based on the X-ray analysis (Table 2), it was clear that the lower-temperature mesophase had rectangular symmetry, although it was not possible to identify the plane group of the Col_r phase, which could be either *p*2*gg* or *c*2*mm*,[12] nor to discriminate the lattice dimensions, due to the presence of only the two fundamental reflections of a rectangular lattice (Table 2 and Table S1). The SmC phase, easily caught on cooling, showed a single reflection corresponding to the layer spacing as well as, for both mesophases, the classical wide-angle broad scattering with a maximum at *ca* 4.4-4.6 Å originating from the average overlapping distances between molten aliphatic chains (h_{ch}) and mesogenic cores (h_c) (Table S1). The mesophase sequence along the series is the same as that observed in the absence of fluorine (**1**-*n* [3]), with only changes in transitions and mesomorphic ranges. Obvious effects of the lateral substitution are: i) the overall 5 to 15 °C decrease in transition temperatures, ii) the persistence of the nematic phase at longer chain lengths and iii) the appearance of the Col_r phase shifted to longer chain lengths, which relates to the steric perturbations introduced in the side-to-side self organisation (see above).

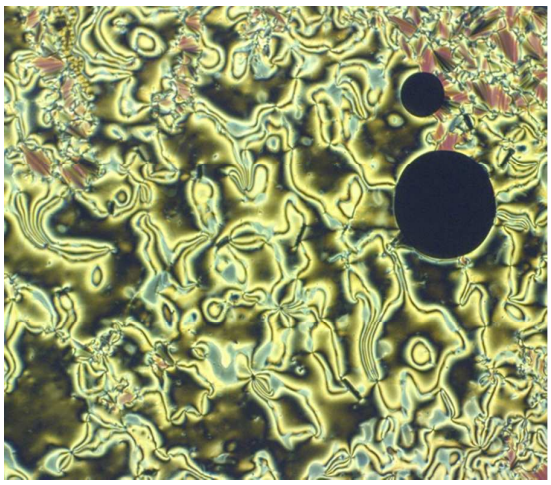
(a)

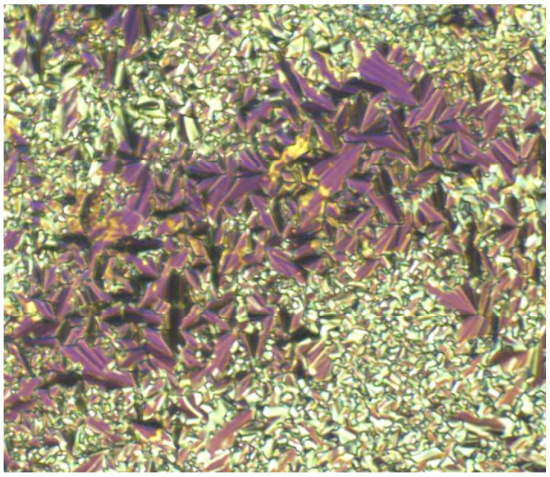
(b)

Figure 3. Optical textures of compound **5**-16 obtained on cooling:
(a) SmC phase at 152 °C and (b) the Col_r phase at 145 °C.

Mesomorphism of series 6

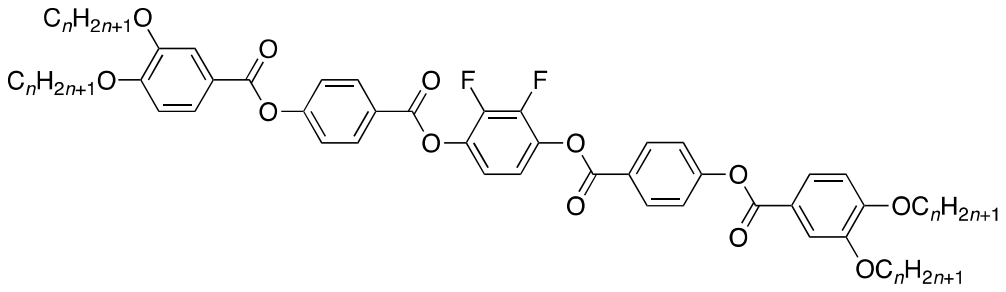

6-*n*

Introduction of two fluorine atoms into the central ring (series **6**-*n*) modifies the mesomorphic properties further according to the same general trend, with in particular the total suppression of the columnar mesophase and the extension of the nematic phase to the whole series. A small decrease in the melting point is also seen, while the clearing points are relatively unaffected leading to an increase (except for **6**-10, which has a higher melting point) in the overall mesophase range compared to the homologues of the series **5**-*n* (Figure 5a). Comparison of homologues within series **6** shows that, with the exception of **6**-10, the SmC range remains practically unchanged as both the Cr-SmC and SmC-N transition temperatures decrease by about the same amount for each pair of methylene groups added. However, the nematic phase is much more dramatically destabilised with increasing chain length reducing from a range of 20.6 °C for **6**-10 to 2.9 °C for **6**-16.

Table 2. X-ray data for the compounds **5**-14, **5**-16, **9**-12, **9**-14, **9**-16, **10**-12 and **10**-14.

Compd	*T*/°C	Phase	V_{mol}/Å^3 (ρ g cm^{-3})[a]	*f*[a]	σ_c/Å^{2,b}	σ_{ch}/Å^{2,b}	$\psi_{c,min}$/°[,c]	h_c/Å[d]	q_{ch}[e]	ψ_{ch}/°[,f]	ψ_c/°[,f]	Phase parameters[g]
5-14	140	SmC	2440 (0.97)	0.675	24.8	46.3	57.6	4.9	1.45	46.5	68.3	d = 36.3 Å; A_{mol} = 67 Å^2
	145	SmC	2448 (0.97)	-	24.9	46.4	57.6	4.9	1.46	46.6	68.4	d = 36.2 Å; A_{mol} = 68 Å^2
	150	SmC	2457 (0.96)	-	25.0	46.6	57.6	4.9	1.47	47.2	68.7	d = 35.8 Å; A_{mol} = 69 Å^2
5-16	135	Col_r	2666 (0.96)	0.703	24.7	46.1	57.6	4.8				a = 76.3 Å; b = 38.3 Å; S = 1461 Å^2; h_{mol} = 1.82; N_c = 4.97
	140	Col_r	2675 (0.95)	-	24.8	46.3	57.6	4.9				a = 76.3 Å; b = 37.9 Å; S = 1445 Å^2; h_{mol} = 1.85; N_c = 4.90
	145	Col_r	2684 (0.95)	-	24.9	46.4	57.6	4.9				a = 75.9 Å; b = 38.1 Å; S = 1448 Å^2;h_{mol} = 1.85; N_c = 4.91
	145	SmC	2684 (0.95)	-	24.9	46.4	57.6	4.9	1.52	48.9	69.4	d = 38.0 Å; A_{mol} = 71 Å^2
9-12	115	SmC	2180 (1.01)	0.636	24.8	45.5	57.0	4.9	1.31	40.0	65.3	d = 36.7 Å; A = 59 Å^2
9-14	135	Col_r	2444 (0.97)	0.671	25.1	46.1	57.0	4.9				a = 76.2 Å; b = 38.2 Å; S = 1456 Å^2; h_{mol} = 1.68; N_c = 5.35
	138	Col_r	2450 (0.97)	-	25.2	46.2	57.0	4.9				a = 76.0 Å; b = 38.1 Å; S = 1448 Å^2; h_{mol} = 1.69; N_c = 5.32
	145	Col_r	2461 (0.97)	-	25.3	46.4	57.0	4.9				a = 75.5 Å; b = 37.6 Å; S = 1419 Å^2; h_{mol} = 1.73; N_c = 5.20
	148	SmC	2466 (0.96)	-	25.3	46.5	57.0	4.9	1.39	44.2	67.0	d = 38.0 Å; A_{mol} = 65 Å^2
9-16	130	Col_r	2670 (0.96)	0.700	25.0	46.0	57.0	4.9				a = 78.6 Å; b = 39.3 Å; S = 1544 Å^2; h_{mol} = 1.73; N_c = 5.19
10-12	150	SmC	2253 (0.99)	0.631	26.0	46.6	56.1	5.0	1.34	41.5	65.3	d = 36.2 Å; A_{mol} = 62 Å^2
	155	SmC	2260 (0.99)	-	26.1	46.8	56.1	5.0	1.34	41.5	65.3	d = 36.2 Å ; A_{mol} = 62 Å^2
10-14	140	Col_h	2473 (0.98)	0.666	25.8	46.3	56.1	5.0				a = 44.2 Å; S = 1694 Å^2; h_{mol} = 1.46; N_c = 3.40
	145	Col_h	2481 (0.98)	-	25.9	46.4	56.1	5.0				a = 44.0 Å; S = 1676Å^2; h_{mol} = 1.48; N_c = 3.36

[a] Molecular volumes, V_{mol}, corresponding densities, ρ (g.cm^{-3}), and chain volume fractions, $f = V_{ch}/V_{mol}$, were determined from reference dilatometric measurements assuming partial molecular volume additivity ($V_{mol} = V_c + V_{ch}$).[13]

[b] σ_c: core cross-section from partial volume assuming core length l_c = 32 Å [$\sigma_c = V_c/l_c = (1-f)V_{mol}/l_c$]
σ_{ch}: chain cross-section [$\sigma_{ch} = 20.915 + 0.0159T$] [13]

[c] $\psi_{c,min} = \arccos(\sigma_c/2\sigma_{ch})$: minimum tilt angle imposed by the ratio of cross-sections of incompatible moieties on both sides of the segregation interface.

[d] $h_c = 0.9763[\sigma_c]^{0.5}$: average lateral distance between rigid cores. [14]

[e] $q_{ch} = A_{mol}/2\sigma_{ch}$: chain packing ratio, *i.e.* degree of stretching of aliphatic chains along smectic layer normal.

[f] $\psi_{ch} = \arccos(1/q_{ch}) = \arccos(2\sigma_{ch}/A_{mol})$: equivalent average chain tilt angle ψ_{ch}. ψ_c: average tilt angle of cores with respect to smectic layer normal, $\psi_c = \arccos(\sigma_c/A_{mol}) = \arccos[(1-f)d/l_c] = \arccos(d_c/l_c)$ (d_c corresponds to the aromatic sub-layer thickness). $\psi_c >> \psi_{c,min}$; $\psi_{ch} >> 0$: which is explained by the contribution of layer undulations effectively predicting the transition to the columnar phase.

[g] For SmC: d is the lamellar periodicity ($d = d_{001}$), and A_{mol} is the molecular area, $A_{mol} = V_{mol}/d$. For Col$_r$: a and b, cell parameters, deduced from the following mathematical expression $1/d_{hk} = [(h/a)^2+(k/b)^2]^{1/2}$; A, lattice area, equal to $a.b$, and S, columnar cross section, which is $A/2$. For Col$_h$: a, hexagonal lattice parameter, $a = 2d_{10}/\sqrt{3}$, and S, columnar cross-section, $S = a^2\sqrt{3}/2$; $h_{mol} = V_{mol}/S$ is the thickness of the volume equivalent to one molecular volume in the column; $N_c = h_{c,col}/h_{mol} = S.h_{c,col}/V_{mol}$: average number of cores per columnar section, where: $h_{c,col} = h_c/\cos\psi_{c,col}$ is the average distance between rigid cores along columns and $\psi_{c,col}$ is the tilt angle of cores out of the columnar lattice plane. In the Col$_r$ phase described previously [15], $\psi_{c,col} \approx 57\pm2° \approx \psi_{c,min}$, $h_{c,col} \approx$ 8.7 Å and $N_c \approx 4.9$. This result confirmed that the break of the smectic layers into ribbons relaxes the layer undulations, but preserves the tilting near the segregration interfaces due to unequal cross sections. For symmetry reasons, this tilt can only be directed along the columnar axis in the Col$_r$ phase, which could be verified by experience. Applying the same approach to the present system gives $\psi_{c,col} \approx \psi_{c,min} \approx$ 56-58° and $h_{c,col} \approx$ 9.0 Å, that leads to N_c values between 4.9 and 5.4, which is very close to the packing parameters of the previous system as expected from the similar rigid core lengths.
In the Col$_h$ phase, with the assumption that molecular clusters are perpendicular to the columnar axis, N_C can be directly deduced using $N_c = S.h_c/V_{mol} \approx$ 3.4.

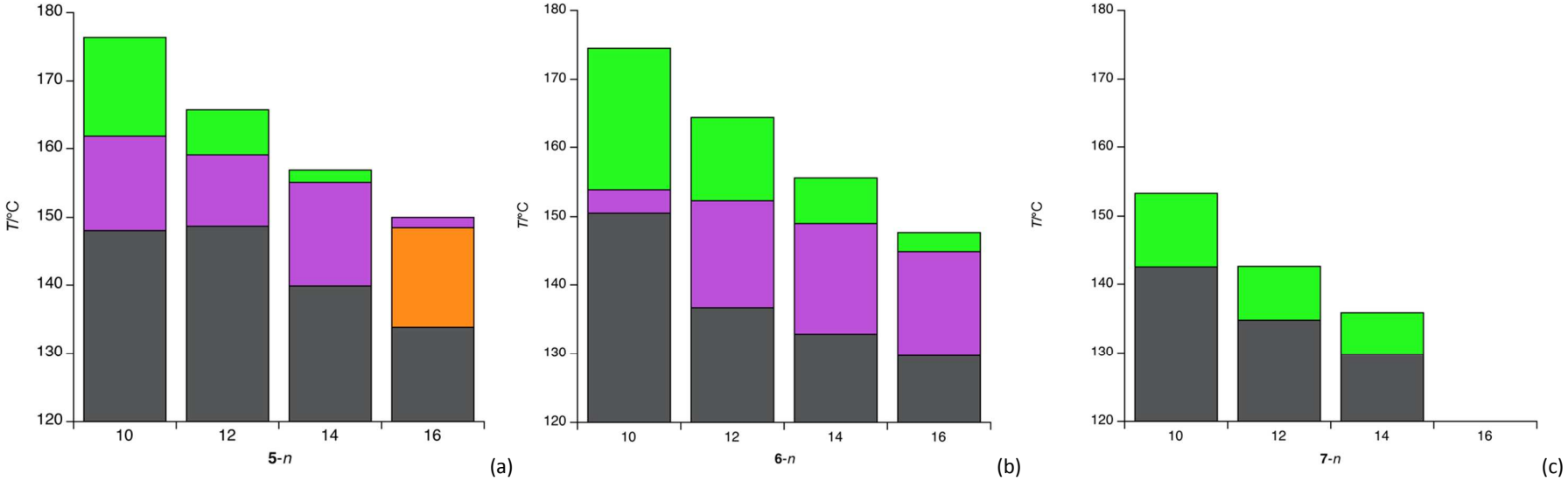

Figure 5. Comparison of mesomorphic behaviour of compounds: (a) **5**-*n*; (b) **6**-*n*; (c) **7**-*n*.

[Grey = Crys; purple = SmC; green = N; orange = Col_r].

Mesomorphism of series 7

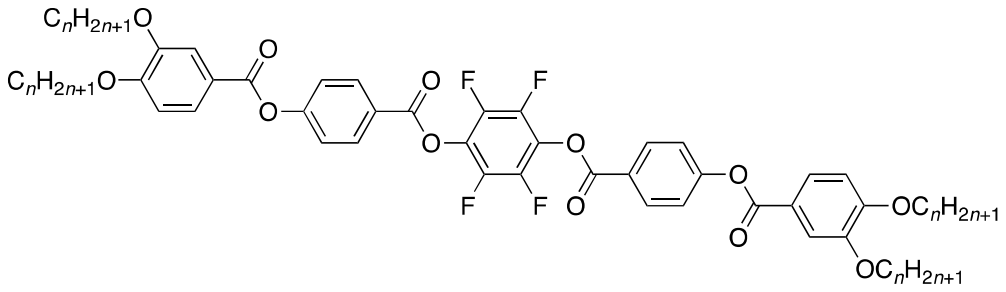

7-*n*

When all four hydrogens of the central phenylene ring were substituted with fluorine atoms, it was found that in all but the longest homologue studied (**7**-14), the only phase observed was nematic with **7**-14 showing a monotropic SmC phase. The obtained data show that the complete fluorination of the central phenylene ring further decreases melting and clearing points. At the same time, mesophase range became narrower as no smectic phase formed and the crystalline phase melted directly into nematic phase, suggesting that the additional fluorine groups further hinder the side-to-side self-organisation of mesogens into layers.

Mesomorphism of series 8

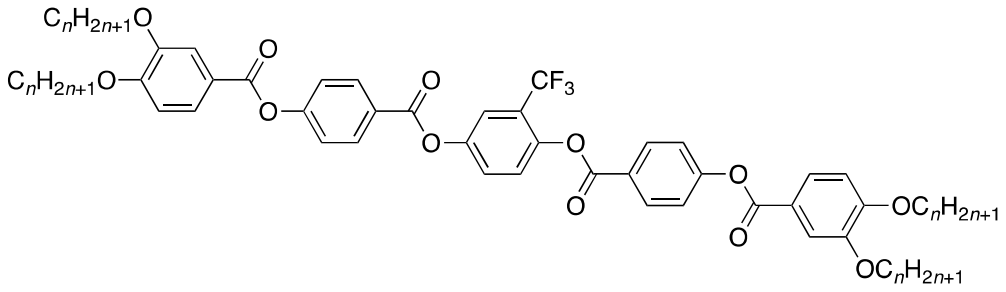

8-*n*

Finally here with fluorinated substituents, three homologues were prepared with a single lateral CF_3 group, **8**-*n*, and showed only a nematic phase, which was enantiotropic for **8**-10 and **8**-12, and (just) monotropic for **8**-14 (Figure 6a). Comparison with the behaviour of the monomethyl-substituted analogues, **2**-*n* (Figure 6b), shows the much greater destabilisation consequent on the

great steric bulk of the fluorinated group. Indeed, in complexes **2** to **4** with lateral methyl groups, steric hindrance led to the complete disappearance of the columnar phase (with respect to unsubstituted **1**), but both the SmC and N phases were still observed, even in the cases of multiple methyl substitutions. [3] The mesomorphic properties were eventually lost totally, or strongly destabilised, when larger lateral groups, such as t-butyl or alkyl chains, were used instead as observed previously [3] and with other related polycatenar mesogens. [16,17,18] This suggests that the dipole moment of the lateral CF_3 polar group is sufficiently strong to stabilise the nematic phase, but its position introduces a steric hindrance in the packing, resulting in the suppression of the smectic phase.

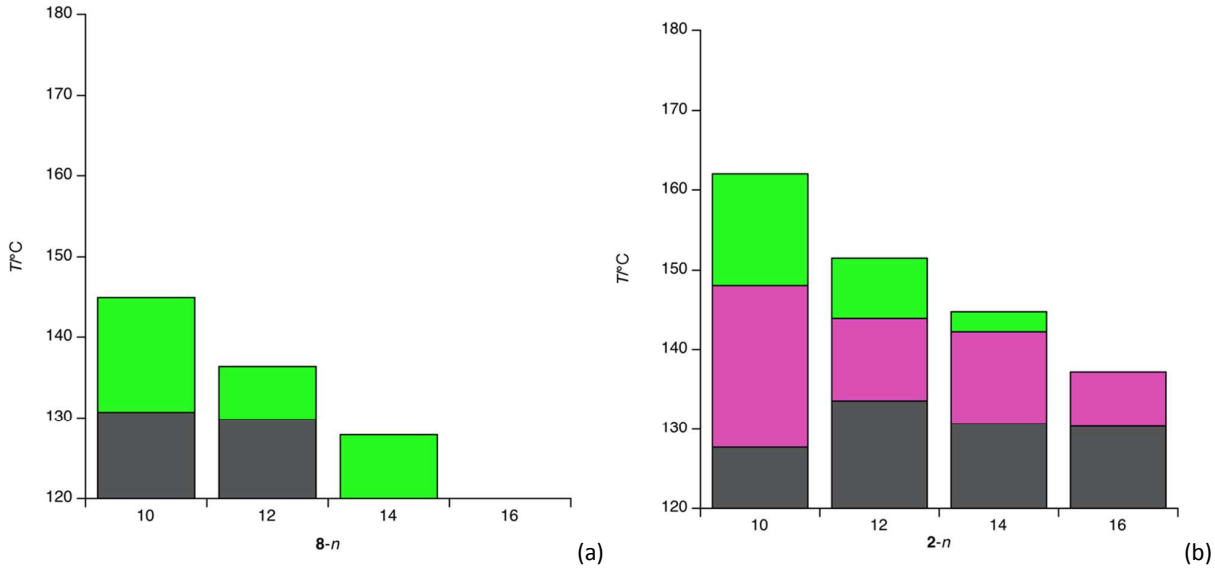

Figure 6. Comparison of mesomorphic behaviour of series (a) **8**-*n* (lateral CF_3) and (b) **2**-*n* (lateral CH_3) [3] [Grey = Crys; purple = SmC; green = N].

Mesomorphism of series 9

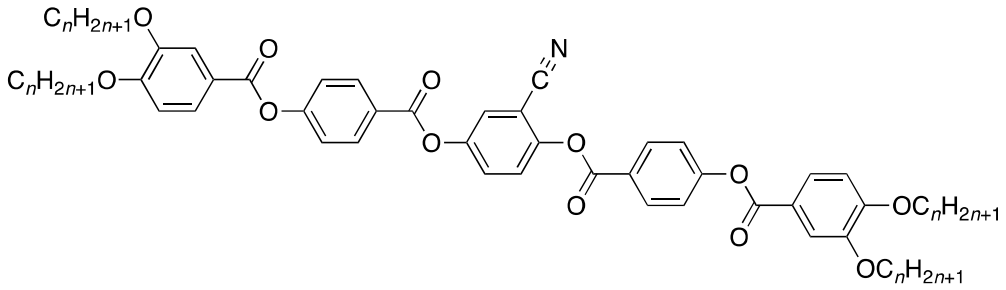

9-*n*

Compounds with one cyano-group in the central phenylene ring display a rich mesomorphism, depending on the length of the aliphatic terminal chains. The shortest-chain homologue prepared, **9**-10, showed both N and SmC phases with the nematic phase disappearing when the chain was elongated slightly as in **9**-12. The next homologue (**9**-14) showed the appearance of a rectangular phase below SmC, whilst for **9**-16, only the rectangular phase was formed. Typical textures are shown as Figure 7. The identity of the phases was confirmed by X-ray analysis, with the (001) reflection being observed for the SmC phase along with the broad wide-angle scattering signal from liquid-like lateral distances. With an estimated molecular length of *ca* 65-70 Å, then the spacing of 36.75 Å represents a tilt angle in the range 55 to 60°. For **9**-14, both phases were found easily and a small increase in the lamellar spacing was seen in the SmC phase consistent with the increase in chain length and the similar tilt angles. The rectangular phase showed two low-angle reflections and, in the absence of higher-order reflections, these could not be assigned unambiguously so that only the most likely is shown in Table 2, whereas the two possible assignments are reported in the Supplementary Information (Table S1). The rectangular nature of the mesophase in **9**-16 was also readily established by X-ray, although as above it was not possible unequivocally to assign the plane group.

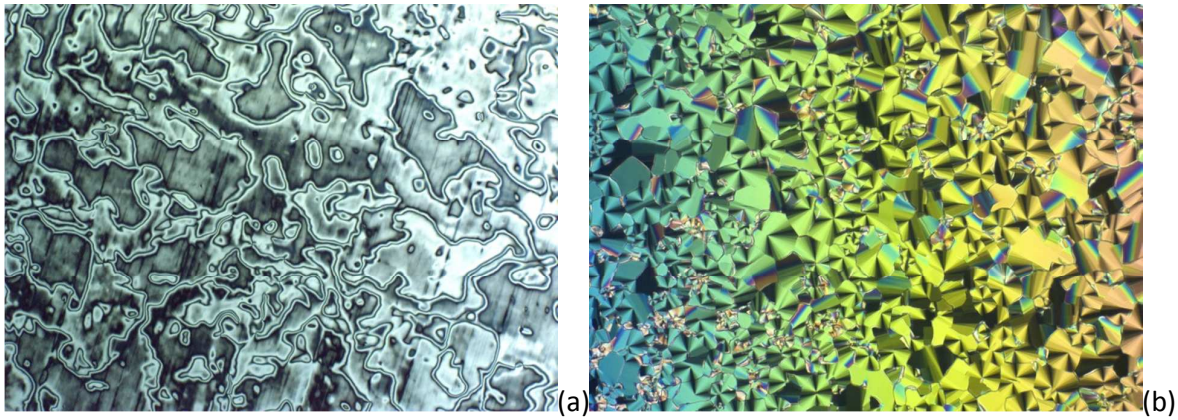

Figure 7. Optical textures, obtained on cooling, of: (a) the SmC phase of **9**-12 at 155 °C; (b) the Col_r phase of **9**-16 at 139 °C.

Mesomorphism of series 10

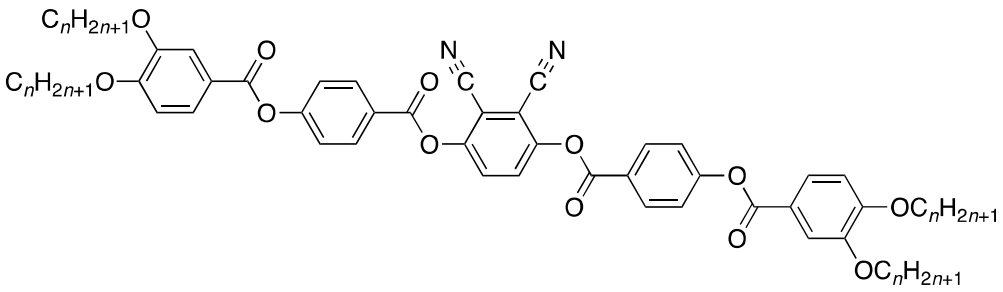

10-*n*

The mesomorphism of this series (Figure 8) evolved in a manner similar to that seen in **9**-*n* so that for **10**-10 both N and SmC phases were seen (Figure 9a), **10**-12 showed only a SmC phase while for **10**-14 only a columnar phase was observed. The textures of the N and SmC phases for **10**-10 and **10**-12 were absolutely characteristic and the X-ray data for **10**-12 were consistent with the presence of a lamellar phase. The tilt angles for **10**-12 is calculated to be all but identical with those of **5**-*n* and **9**-*n*.

For **10**-14, the optical texture (Figure 9b) is indicative of a columnar phase. X-ray analysis helps to discriminate, since only a single reflection is seen, which excludes the possibility of a rectangular phase. On this basis, the phase is assigned as Col_h as the texture, although not well developed, is

consistent with a Col_h phase and not consistent with other possibilities (*e.g.* lamello-columnar) that might also show a single reflection.

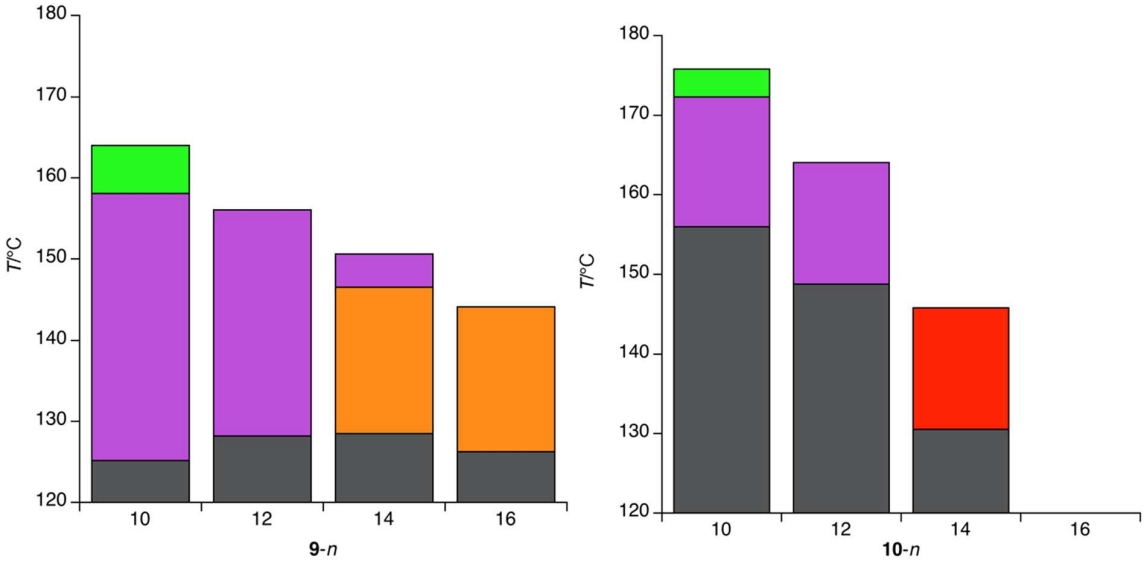

Figure 8. Thermal behaviour for compounds of series **9**-*n* and **10**-*n*.

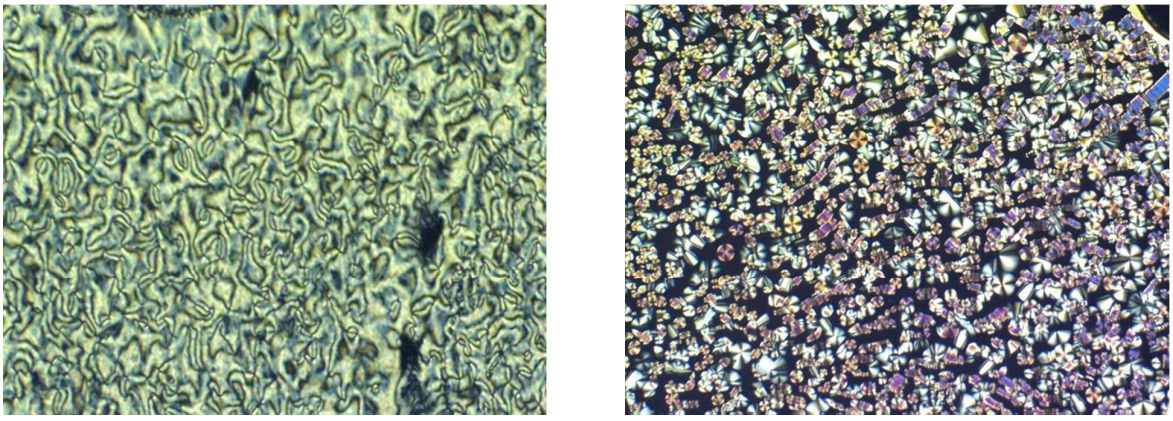

Figure 9. Optical texture of: (a) **10**-10 on cooling at 167 °C; (b) **10**-14 at 143 °C on cooling.

Discussion

It is useful to begin by recalling the mesomorphism of the parent compounds **1**-*n*, with no substituents on the central phenyl ring. Their phase diagram is found as Figure S1 where it is shown alongside those of **5**-*n* to **10**-*n* for purposes of comparison. The compounds melt around

150 °C and the shorter-chain homologues (*n* = 10, 12) show both a SmC and a nematic phase – typical for this kind of symmetric, tetracatenar mesogen.[1,2] For *n* = 14, the nematic phase disappears and a phase with rectangular symmetry is seen below the SmC phase. The SmC phase disappears at *n* = 16. Typically for many tetracatenar mesogens, increasing chain length leads to the formation of a Col_h phase observed above the SmC phase, which is a reflection of the effect of increased terminal chain volume as discussed extensively elsewhere.[19,20,21,22,23,24,25,26,27] Here the new phase at longer chain lengths is below the SmC and, by analogy, it is tempting to label it as Col_r (as done earlier in the paper and extensively in the literature). Of course, in polycatenar mesogens, it is rarely if ever the case that X-ray studies show a stacking period and indeed some of us have shown previously [12,28] that it is rarely appropriate to think of simple, well-defined 'slices' of a column containing a finite number of discrete molecules in the way proposed originally when these materials were first discovered.[29] We feel, therefore, that it may not be helpful simply to label this phase as Col_r, rather that it may be better simply to regard it as a ribbon phase that is somehow analogous to the SmÃ [30] and B_1 [31] phases, which also possess rectangular symmetry. Such a classification would then make no presumptions as to the columnar nature of the arrangement. Nonetheless, to avoid a random expansion in phase nomenclature we stay with the label Col_r, but note that this will, in due course, require addressing.

Then looking first to the mono- (**5**-*n*) and di- (**6**-*n*) fluoro derivatives, it is seen that there is a progressive destabilisation of the crystal phase with increasing *n* and an analogous decrease in the clearing point. The degree of destabilisation is all but independent of the number of lateral fluorine atoms here and on average the clearing points for **5**-*n* and **6**-*n* are about 10 °C below those of **1**-*n*. However, the more significant difference is the gradual suppression of the rectangular ribbon phase, which is absent totally in **6**-*n* and present in only the longest homologue in series **5**-*n*. For these materials, two factors become important. One is the fact that F is somewhat larger in radius (16%) than H while in addition the C–F bonds add a dipole moment (**5**-*n* and **6**-*n*). The effect of lateral dipole moments on the mesomorphism of such tetracatenar mesogens is effectively unexplored and the possible effect will be considered later.

By comparison, the behaviour of the tetrafluorophenyl materials (**7**-*n*) shows slightly great destabilisation of the crystal phase, elimination of all phases other than nematic and a clearing point destabilisation of around 30 °C. Studies by Matharu *et al.* have shown previously that heavily fluorinated aromatic cores do tend to destabilise mesophase clearing points and promote nematic phases on the basis that tetrafluorophenyl units suppress the side-to-side organisation required for formation of lamellar phases.[32] The difference then with **5**-*n* and **6**-*n* is that they are dipolar in nature, a point that will be discussed later.

Use of CF_3 as lateral substituent (**8**-*n*) also introduces a dipole moment, but more importantly significant steric bulk so that there is even great destabilisation of the mesophase (unsurprisingly only a nematic phase is seen) to the point where it is monotropic in **8**-14. The steric nature of the destabilisation is emphasised in Figure 6 where there is comparison with the analogous compound with a single lateral methyl group (**2**-*n*).

In considering the cyano-substituted materials, it can be seen that the lower-symmetry, mono-substituted homologues (**9**-*n*) show significant destabilisation of the crystal phase analogous to that seen for $–CF_3$ but in this case the mesomorphism is much less affected. Thus while the temperatures have changed a little, the nematic phase is lost in **9**-12 and the mesomorphic ranges are greater, the behaviour of **9**-*n* looks a lot like that of **1**-*n*. However, addition of the second cyano group (**10**-*n*) stabilises the crystal phase compared to the other substituted compounds and offers a significant stabilisation over **9**-*n*. In common with **9**-*n*, a nematic phase is seen only for **10**-10 and a hexagonal phase (as opposed to rectangular) appears at **10**-14 in which compound the SmC phase is absent. What these data suggest is that first the mesophases are stabilised by the strong lateral dipole induced by the presence of the cyano group(s), which is significantly stronger than that induced by fluorine incorporation (*e.g.* dipole moments of fluorobenzene and cyanobenzene are 1.66 and 4.28 D, respectively). Secondly, it is likely that these strong lateral dipole moments cause a degree of self-association that would appear to stabilise the columnar phases. The fluoro-substituted materials **5**-*n* and **6**-*n* evidently do not possess a strong enough

dipole moment to allow this to happen and so the major effect is steric. This is supported by the observation of a ribbon phase for **5**-*n* and not **6**-*n*.

In further consideration of the rectangular phase, it was noted earlier that X-ray diffraction in the mesophases of **5**-16 revealed the presence of both a SmC phase and a rectangular phase and that the precise plane group symmetry of the latter (choice between *p*2*gg* and *c*2*mm* [12]) was not apparent owing to the absence of higher-order reflections that would show systematic absences. However, consideration of the data in Table S1 shows that the periodicity of the (20) reflection (first indexation) is the same as that of the (001) reflection of the SmC phase directly above it. Furthermore, the enthalpy change between the two is rather small. It becomes apparent that a simple tilt in the *c*2*mm* phase could lead to a SmC phase where *d*(001) was the same as *d*(20) of the rectangular phase.[12] On this basis we offer a tentative assignment of the rectangular phase as having *c*2*mm* symmetry, which would also be consistent with the generally held practice of assigning the plane group to be the higher-symmetry phase in cases where there is a choice.

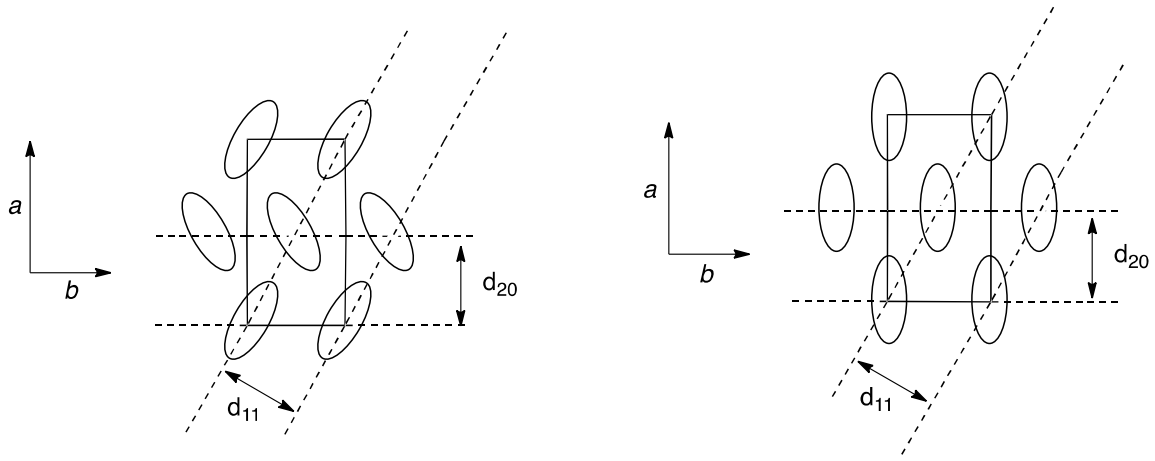

Figure 10. The *p*2*gg* (left) and *c*2*mm* (right) plane groups showing the origin of the (11) and (20) reflections.

The Nature of the SmC Phase

The observation of the SmC phase in polycatenar mesogens is usually (and correctly) attributed to the mismatch in cross-sectional area between the (normally) rigid, elongated core and that of the two terminal chains at each end of the molecule. This phenomenon is well understood and leads to the idea of a core tilt angle, ψ_c, and a chain tilt angle, ψ_{ch} (these quantities are as defined in the footnote of Table 2). Both of these angles are in the plane that contains the tilted molecule and it is regarded that there is effectively no chain (or core) tilt out of that plane, hence the layers have C_{2h} symmetry. The lamellar structure obviously presupposes that tilted cores and molten chains form continuous sub-layers.

From dilatometric data and from the parameters obtained from the X-ray measurements carried out on these materials, it is possible to analyse the SmC phase further. The molecular volume, V_{mol} is obtained readily and, knowing the layer spacing, d, it is possible simply to compute the effective molecular area, $A_{mol} = V_{mol}/d$. Consideration of the interface between the core and the chains in the molecule, generated by the alternation of sub-layers of core and chains, suggests, in line with previous derivations, that in the SmC phase of polycatenar mesogens, $A_{mol} \approx 2\sigma_{ch}$.

Such a tilting of mesogens that expands A_{mol} to the cross section of both stretched chains has been observed when no columnar phase was associated with the SmC phase. [33] Even in such an archetypical situation, significant discrepancies between the two areas may however been encountered, as, for instance, for a closely related tetracatenar for which A_{mol} was found to be some 10-15% greater than $2\sigma_{ch}$, which was related to the angle between direction of elongation of the chains and the layer normal. [13] In the presence of columnar phases in the phase diagram, it is observed that discrepancies are more substantial and values of A_{mol} can be as much as 35% greater than $2\sigma_{ch}$, if a Col_h phase were in the phase sequence, [20] and up to 47% greater in the present materials where there is a Col_r phase (*e.g.* for the SmC phase of **5**-14 at 145 °C, A_{mol} = 68 Å^2 while $2\sigma_{ch}$ = 46.4 Å^2; Table 2). It is also possible to extract a core tilt angle from the data (ψ_c = arcos{σ_c/A_{mol}}) which, depending on the temperature, comes out in the region 65-70°; this is rather large.

In order to accommodate this significant area mismatch, it is necessary to consider how space may be filled most efficiently and at lowest energy cost. In fact space may be filled effectively if it assumed both that (i) there is undulation of the layers and (ii) the chain volume spreads laterally so that some chain volume from one molecule will compensate part of A_{mol} of a neighbouring molecule (recall that the chain volume approximates to a cone emanating from the core-chain interface). The picture obtained is then one of a heavily tilted molecular core whose area is matched at the core-chain interface by terminal chains that would spontaneously deviate from the layer normal by an average angle of 47° implying the creation of free volume. Clearly such a situation cannot pertain since interfaces are costly in energy and their extension spontaneously reduces to a minimum, so that the additional lateral expansion in reality reveals a contribution to layer undulations that in effect predict a transition to a columnar phase.

In now addressing the Col_r-to-SmC transition, the process comes down to the fusion of the ribbons into continuous sub-layers and the accompanying transformation of the row periodicity (d_{20}) into the lamellar periodicity, d (Figure 11). Coincidence between d_{20} and the lamellar period, d, is indeed observed, leading to the definition of an average tilt angle, $\psi_{c,mean}$, which is preserved during the transition. In the SmC phase, it holds simply that $\psi_{c,mean}=\psi_c$, while in the Col_r phase, $\psi_{c,mean}$ is larger than the effective tilt angle of mesogens within the ribbons, $\psi_{c,col}$, due to the contribution of aliphatic region (Figure 11). In this context, $\psi_{c,col}$ likely stays close to the minimum angle $\psi_{c,min}$ which would just allow the core cross-section to be matched by chain cross-section (see footnote of Table 2), and the high ψ_c values in the SmC phase are the consequence of the evolution of the strongly tilted mesogens from ribbons to lamellae. In other words, the alternation of ribbons and spacings in the Col_r phase is smoothed to a modulation that mimics a sequence of flat sub-layers with high tilt angles ψ_c and ψ_{ch}. Depending upon the amplitude of the modulation, these angles depart more or less from $\psi_{c,min}$ and zero, explaining the wide-range of values encountered.

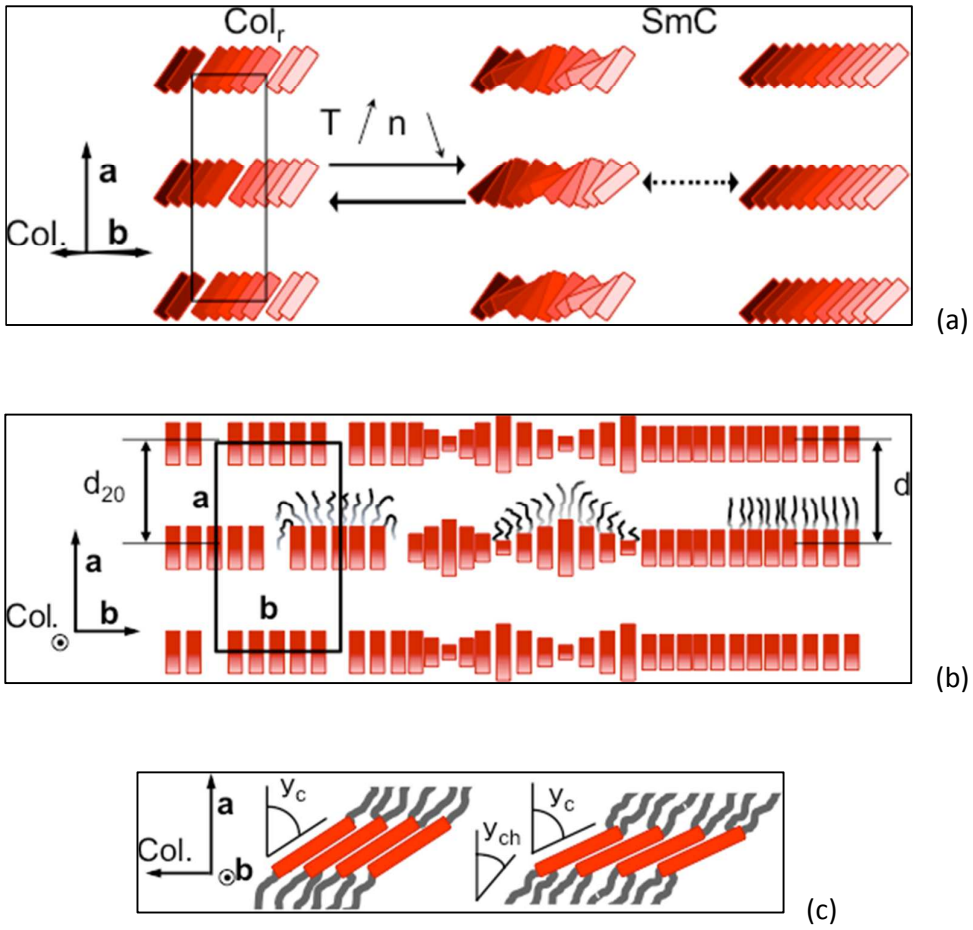

Figure 11 From left to right, schematic representation of the Col_r, undulating SmC and SmC phases (with and without a columnar phase in the phase sequence, and with the emphasis put on the evolution of the mesogen tilting between the Col_r and SmC phases. (a) Perspective view of the three mesophases; (b) projection onto the rectangular lattice plane, mesogen and chains tilts; (c) description of the chains and core angles in both phases, respectively.

Conclusions

The present work shows once more the way in which the mesomorphism of simple tetracatenar mesogens is influenced by the presence of lateral substituents. The evidence suggests that where there is a strong, lateral dipole moment then self-association can stabilise the mesophases against steric disturbance and help retain columnar phases. However, where there are much weaker dipole moments then steric effects predominate, which act to destabilise columnar phases. Where substituents are weakly dipolar and sterically large (–CF_3) then the destabilisation is significant.

Detailed consideration of structural factors obtained from X-ray measurements and volume parameters from a database compiled from previous studies reveals that in the SmC phase there is a very large core tilt angle. Furthermore, the effective molecular area, A_{mol}, cannot be compensated by chain cross-section at the core-chain interface leading to proposal of a model where core volume is compensated by chain volume from neighbouring molecules, possible because of the cone-like extension of the terminal chain volume. The model also necessitates layer undulation, which is then related to the appearance of a columnar phase within the mesomorphic sequence. These results mirror those from earlier studies of and allow a common picture of the mesomorphism, phase structure and factors influencing phase transitions in polycatenar systems.

Experimental

General

Polarising optical microscopy was performed on microscope Leitz Laborlux 12 Pol fitted with Mettler heating stage FP90.

The transition temperatures were determined by a differential scanning calorimetry (DSC) was on Mettler DSC822^e (running on the Star^e software which is equipped with an autosampler). The measurements were carried out three times to reproducibility of the results with the heating/cooling rate 10 K min^{-1}. DSC data mentioned in this article are onset temperatures.

The SAXS patterns were obtained with a transmission Guinier-like geometry. A linear focalised monochromatic Cu-Kα_1 beam (λ = 1.5405Å) was obtained using a sealed-tube generator (600 W) equipped with a bent quartz monochromator (both generator and monochromator were manufactured by Inel). In all cases, the crude powder was filled in Lindemann capillaries of 1 mm diameter and 10 μm wall-thickness. The diffraction patterns were recorded with a curved Inel

CPS120 counter gas-filled detector linked to a data acquisition computer (periodicities up to 70 Å) and on image plates scanned by STORM 820 from Molecular Dynamics with 50 μm resolution (periodicities up to 120 Å). The sample temperature was controlled within ±0.01 °C and exposure times were varied from 1 to 24 h.

Compounds were characterised by ^{1}H NMR spectroscopy using a Jeol JNM-EX 270 FT NMR system at 270 MHz for ^{1}H NMR, while elemental analysis was carried out at the University of Newcastle.

Synthesis

2-Fluorohydroquinone, 2,3-difluorohydroquinone [34], 2-cyanohydroquinone [35] and 2-(trifluoromethyl)hydroquinone [36] were prepared as described in the literature.

General Procedure for the Synthesis of Tetracatenar compounds (**5**-*n* to **10**-*n*):

The appropriate 4-(3,4-dialkoxybenzoyloxy)benzoic acid (1.5 mmol), the required hydroquinone (0.8 mmol), dicyclohexylcarbodimide (DCC, 2 mmol) and 4-(*N,N*-dimethylamino)pyridine (~40 mg) were stirred in dry dichloromethane (50 cm^{3}) under a nitrogen atmosphere for 24 h. The resulting mixtures were purified by flash column chromatography over silica gel (60 μm), using dichloromethane as the eluent. Analytical data are collected in Table 3.

Table 3 Analytical data for compounds **5**-*n* – **10**-*n*

Compound	Yield/%	Calculated (Found)/%		
		C	H	N
5-10	47	74.0(74.3)	8.5 (8.5)	
5-12	61	75.0 (74.9)	9.0 (8.9)	
5-14	59	75.8 (76.1)	9.4 (9.6)	
5-16	7	76.5 (76.3)	9.8 (10.1)	
6-10	62	72.9 (72.9)	8.3 (7.9)	

6-12	73	74.0 (74.2)	8.8 (9.0)	
6-14	19	74.9 (74.9)	9.2 (9.2)	
6-16	5	75.6 (75.9)	9.6 (9.5)	
7-10	26	70.8 (70.9)	7.9 (7.9)	
7-12	33	72.0 (72.0)	8.4 (8.7)	
7-14	52	73.0 (73.2)	8.9 (8.9)	
8-10	40	72.0 (71.9)	8.1 (8.4)	
8-12	35	73.1 (73.3)	8.7 (9.0)	
8-14	30	74.1 (74.2)	9.1 (9.1)	
9-10	43	74.5 (74.6)	8.4 (8.6)	1.2 (1.3)
9-12	71	75.5 (75.6)	8.9 (9.1)	1.1 (1.2)
9-14	30	76.3 (76.3)	9.35 (9.44)	0.98 (0.85)
10-10	26	74.0 (74.3)	8.2 (8.2)	2.3 (2.5)
10-12	8	75.0 (74.5)	8.7 (8.6)	2.1 (2.1)
10-14	3.5	75.8 (76.0)	9.1 (9.3)	1.9 (2.2)

Indicative ^{1}H NMR data:

5-*n*: ^{1}H NMR (400 MHz; $CDCl_3$): 8.3-8.25 (4H, m); 7.8 (2H, dd); 7.7 (2H, d); 7.38–7.34 (4H, m); 7.3 (1H, m); 7.2 (1H, m); 7.1 (1H, m); 6.9 (2H, d); 4.0 (8H, dt), 1.9 (8H, m); 1.5–1.3 (56–104 H, m); 0.9 (12H, m)

6-*n*: ^{1}H NMR (400 MHz; $CDCl_3$): 8.3 (4H, m); 7.8 (2H, dd); 7.7 (2H, d); 7.4 (4H, m); 7.1 (2H, m); 6.9 (2H, d); 4.0 (8H, dt), 1.9 (8H, m); 1.5–1.3 (56-104 H, m); 0.9 (12H, m).

7-*n*: ^{1}H NMR (400 MHz; $CDCl_3$): 8.3 (4H, m); 7.8 (2H, dd); 7.7 (2H, d); 7.4 (4H, m); 6.9 (2H, d); 4.0 (8H, dt), 1.9 (8H, m); 1.5–1,3 (56–88H, m); 0.9 (12H, m).

8-*n*: ^{1}H NMR (400 MHz; $CDCl_3$): 8.3 (4H, m); 7.8 (2H, dd); 7.65 (2H, d); 7.6 (1H, d); 7.5 (2H, m); 7.4 (4H, m); 6.9 (2H, d); 4.0 (8H, dt), 1.9 (8H, m); 1.5–1,3 (56–88H, m); 0.9 (12H, m).

9-*n*: ^{1}H NMR (400 MHz; $CDCl_3$): 8.3 (4H, m); 7.8 (2H, m); 7.7-7.5 (5H, m); 7.4 (4H, m); 6.9 (2H, d); 4.0 (8H, dt), 1.9 (8H, m); 1.5–1,3 (56–104H, m); 0.9 (12H, m).

10-*n*: ^{1}H NMR (400 MHz; $CDCl_3$): 8.3 (4H, m); 7.8 (4H, m); 7.64 (2H, d); 7.4 (4H, m); 6.9 (2H, d); 4.0 (8H, dt), 1.9 (8H, m); 1,5 –1.3 (56–88 H, m); 0.9 (12H, m).

Acknowledgements

We thank the EU Marie Curie programme for a fellowship (AIS), the Royal Society for a Joint Project Grant. BD and BH thank CNRS and Université de Strasbourg for support.

REFERENCES

[1] J. Malthête, H. T. Nguyen and C. Destrade, *Liq. Cryst.*, 1993, **13**, 171–187.

[2] H. T. Nguyen, C. Destrade and J. Malthête, *Adv. Mater*., 1997, **9**, 375-388.

[3] A. I. Smirnova, N. V. Zharnikova, B. Donnio and D. W. Bruce, *Russ. J. Gen. Chem*., 2010, **80**, 1331-1340 (*Zh. Obsh. Khim*. 2010, **80**, 1165-1174). Erratum *Russ. J. Gen. Chem*., 2010, **80**, 2223.

[4] M. Hird and K. J. Toyne, *Mol. Cryst., Liq. Cryst*., 1998, **323**, 1–67.

[5] M. Hird, *Chem. Soc. Rev*., 2007, **36**, 2070-2095.

[6] M. Bremer, P. Kirsch, M. Klasen-Memmer and K. Tarumi, *Angew. Chem. Int. Ed*. 2013, **52**, 8880 – 8896.

[7] J. W. Goodby, I. M. Saez, S. J. Cowling, J. S. Gasowska, R. A. MacDonald, S. Sia, P. Watson, K. J. Toyne, M. Hird, R. A. Lewis, S.-E. Lee and V. Vaschenko, *Liq. Cryst*., 2009, **36**, 567-605.

[8] D. A. Dunmur and K. Toriyama, *Mol. Cryst., Liq. Cryst*., 1991, **198**, 201-213.

[9] K. Toriyama, D. A. Dunmur and S. E. Hunt, *Liq. Cryst*., 1989, **5**, 1001-1009.

[10] D. A. Dunmur and P. Palffy-Muhoray, *Mol. Phys*., 1992, **76**, 1015-1023.

[11] R. P. Tuffin, K. J. Toyne and J. W. Goodby, *J. Mater. Chem*., 1996, **6**, 1271-1282.

[12] B. Donnio, B. Heinrich, H. Allouchi, J. Kain, S. Diele, D. Guillon and D. W. Bruce, *J. Am. Chem. Soc.*, 2004, **126**, 15258–15268.

[13] A. C. Ribeiro, C. Cruz, H. T. Nguyen, S. Diele, B. Heinrich and D. Guillon, *Liq. Cryst*., 2002**, 29**, 635-640.

[14] M. Marcos, R. Giménez, J. L. Serrano, B. Donnio, B. Heinrich and D. Guillon, *Chem. Eur. J*., 2001, **7**, 1006-1013.

[15] A. C. Ribeiro, B. Heinrich, C. Cruz, H. T. Nguyen, S. Diele, M. W. Schröder and D. Guillon, *Eur. Phys J. E*., 2003, **10**, 143-151.

[16] B. P. Hoag and D. L. Gin, *Adv. Mater*., 1998, **10**, 1546-1551.

[17] A. Pérez, J. L. Serrano, T. Sierra, A. Ballesteros, D. de Saá, R. Termine, U. Kumar Pandey, A. Golemme, *New J. Chem*., 2012, **36**, 830–842.

[18] C. P. Roll, B. Donnio, W. Weigand and D. W. Bruce, *Chem. Commun*., 2000, 709-710.

[19] B. Donnio and D. W. Bruce, *J. Chem. Soc., Dalton Trans*., 1997, 2745-2755.

[20] D. Guillon, B. Heinrich, A. C. Ribeiro, C. Cruz and H. T. Nguyen, *Mol. Cryst., Liq. Cryst*., 1998, **317**, 51-64.

[21] K. E. Rowe and D. W. Bruce, *J. Mater. Chem*., 1998, **8**, 331-341.

[22] D. Fazio, C. Mongin, B. Donnio, Y. Galerne, D. Guillon and D. W. Bruce, *J. Mater. Chem*., 2001, **11**, 2852-63.

[23] A. I. Smirnova, D. Fazio, E. Fernandez Iglesias, C. G. Hall, D. Guillon, B. Donnio and D. W. Bruce, *Mol. Cryst., Liq. Cryst*., 2003, **396**, 227-240.

[24] R. W. Date, E. Fernandez Iglesias, K. E. Rowe, J. M. Elliott and D. W. Bruce, *Dalton Trans*., 2003, 1914–1931.

[25] C . Fang He, J. Richards Gary, S. M. Kelly, A. E. A. Contoret and M. O'neill, *Liq. Cryst*., 2007, **34**, 1249-1267.

[26] T. Cardinaels, J. Ramaekers, P. Nockemann, K. Driesen, K. Van Hecke, L. Van Meervelt, G. Wang, S. De Feyter, E. Fernandez Iglesias, D. Guillon, B. Donnio, K. Binnemans and D. W. Bruce, Soft Matter, 2008, **4**, 2172-2185.

[27] S. Suarez, O. Mamula, R. Scopelliti, B. Donnio, D. Guillon, E. Terazzi, C. Piguet and J. C. Bünzli, *New J. Chem.,* 2005, **29**, 1323-1334.

[28] C. Domínguez, B. Donnio, S. Coco and P. Espinet, *Dalton Trans*., 2013, **42**, 15774-15784.

[29] J. Malthête, A.-M. Levelut and H. T. Nguyen, *J. Phys. Lett. (Paris)*, 1985, **46**, 875-880.

[30] See *e.g.*: M. Šepelj, A. Lesac, U. Baumeister, S. Diele, H. L. Nguyen and D. W. Bruce, *J. Mater. Chem.*, 2007, **17**, 1154-1165.

[31] For reviews of bent-core mesogens see: (a) G. Peltz, S. Diele and W. Weissflog, *Adv. Mater.*, 1999, **11**, 707-724; (b) R. A. Reddy and C. Tschierske, *J. Mater. Chem.*, 2006, **16**, 907-961; (c) N. Vaupotic, D. Pociecha and E. Gorecka, *Top. Curr. Chem.*, 2012, **318**, 281-302.

[32] See e.g. A. S. Matharu, R. C. Wilson and D. J. Byron, *Liq. Cryst*., 1997, **23**, 575-588.

[33] H. Allouchi, M. Cotrait, D. Guillon, B. Heinrich and H. T. Nguyen, *Chem. Mater*., 1995, **7**, 2252-2258.

[34] M. Essers and G. Haufe, *J. Chem. Soc., Perkin Trans. 1*, 2002, 2719-2728.

[35] K. Wallenfels, D. Hofmann and R. Kern, *Tetrahedron*, 1965, **21**, 2231-2237.

[36] A. E. Feiring and W. A. Sheppard, *J. Org. Chem.*, 1975, **40**, 2543-2545.